EUROPEAN ORGANIZATION FOR NUCLEAR RESEARCH

Proposal to the ISOLDE and Neutron Time-of-Flight Committee
(April 23, 2007)

INVESTIGATION OF THE PROTON-NEUTRON INTERACTION BY HIGH-PRECISION NUCLEAR MASS MEASUREMENTS

D. Beck[1], K. Blaum[1,2], M. Breitenfeldt[3], S. George[1,2], F. Herfurth[1], A. Herlert[4], A. Kellerbauer[5], H.-J. Kluge[1], M. Kowalska[4], D. Lunney[6], S. Naimi[6], D. Neidherr[2], R. Savreux[1], S. Schwarz[7], L. Schweikhard[3], C. Weber[8], C. Yazidjian[1], B. Akkus[9], R.B. Cakirli[9,10], R.F. Casten[10]

[1]GSI, Planckstraße 1, 64291 Darmstadt, Germany
[2]Institut für Physik, Johannes Gutenberg-Universität, 55099 Mainz, Germany
[3]Institut für Physik, Ernst-Moritz-Arndt-Universität, 17487 Greifswald, Germany
[4]CERN, Physics Department, 1211 Geneva 23, Switzerland
[5]MPI für Kernphysik, Saupfercheckweg 1, 69117 Heidelberg, Germany
[6]CSNSM-IN2P3-CNRS, Université de Paris Sud, 91406 Orsay, France
[7]NSCL, Michigan State University, East Lansing, Michigan 48824-1321, USA
[8]Department of Physics, University of Jyväskylä, 40014 Jyväskylä, Finland
[9]Department of Physics, Istanbul University, Turkey
[10]WNSL, Yale University, New Haven, Connecticut 06520-8124, USA

Spokesperson: Magdalena Kowalska (*magdalena.kowalska@cern.ch*)
Local Contact: Alexander Herlert (*alexander.herlert@cern.ch*)

CERN-INTC-2007-019+INTC-P-230
23 April 2007

Abstract

We propose to measure the atomic masses of a series of short-lived nuclides, including ^{70}Ni, $^{122\text{-}130}$Cd, ^{134}Sn, ^{138,140}Xe, $^{207\text{-}210}$Hg, and $^{223\text{-}225}$Rn, that contribute to the investigation of the proton-neutron interaction and its role in nuclear structure. The high-precision mass measurements are planned for the Penning trap mass spectrometer ISOLTRAP that reaches the required precision of 10 keV in the nuclear mass determination.

Introduction and motivation:

The structural evolution in atomic nuclei as a function of the neutron number N and the proton number Z can be largely understood as a result of proton-neutron (p-n) interactions. The p-n interaction also plays an important role for the development of configuration mixing, the onset of collectivity and ellipsoidal shapes in nuclei, single-particle energies and magic numbers, and the microscopic origins of quantum-phase-transitions in the geometrical shapes of atomic nuclei [1-3].

The sum of all nucleonic interactions is reflected by the binding energies. While single differences of binding energies give separation energies, double differences of binding energies can isolate specific classes of interactions. One of them is the average interaction of the last two protons and the last two neutrons, δV_{pn}, for even-even nuclei [4], which is given by the following double difference equation:

$$\delta V_{\rm pn}\,(Z,N) \;=\; ¼\,[\;\{BE(Z,N) - BE(Z,N\text{-}2)\} - \{BE(Z\text{-}2,N) - BE(Z\text{-}2,N\text{-}2)\}\;], \qquad (1)$$

where the binding energy BE is defined as:

$$BE(Z,N) \;=\; [(Nm_{\rm n} + Zm_{\rm p} - m(Z,N)\,]\,c^2. \qquad (2)$$

Thus, to calculate $\delta V_{\rm pn}$ values, the corresponding nuclear masses $m(Z,N)$ are required.

The first investigation on $\delta V_{\rm pn}$ by J.-Y. Zhang *et al.* in 1988 [4] was extended after the latest Atomic-Mass Evaluation (AME) in 2003 [5] which allowed to calculate many more $\delta V_{\rm pn}$ values [6,7]. These studies published in Phys. Rev. Lett. revealed a number of interesting results such as evidence for an empirical correlation between $\delta V_{\rm pn}$ values and growth rates of collectivity [8], and intriguing patterns in specific regions of the nuclear chart.

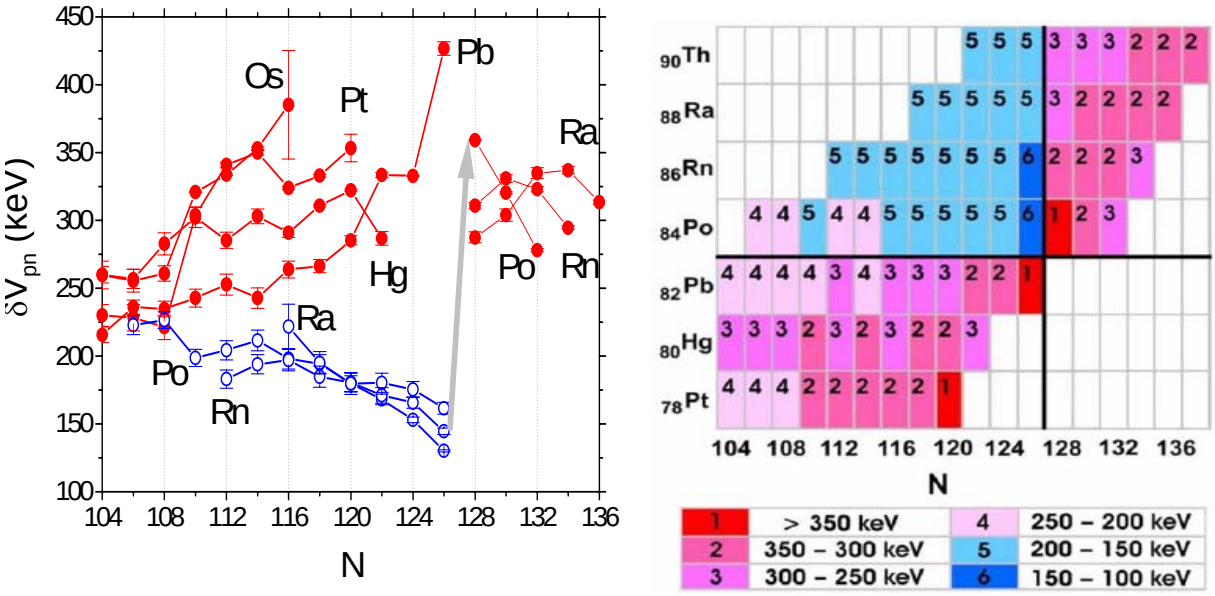

Figure 1: Left: Empirical $\delta V_{\rm pn}$ values for the ^{208}Pb region. Red and blue colors emphasize changes in $\delta V_{\rm pn}$ depending on the *nl* values in the proton and neutron orbits, respectively. The gray arrow shows the sudden jump at N=128 (based on Ref. 6). Right: Color coded $\delta V_{\rm pn}$ values in a Z-N chart for the same nuclei as in the left-hand side figure (based on Ref. 6).

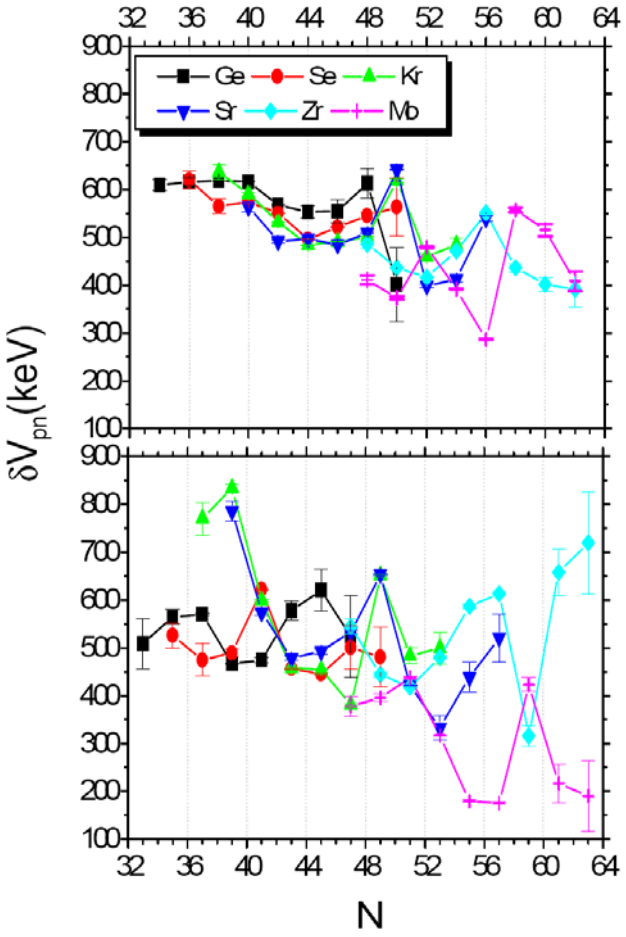

Figure 2: Empirical δV_{pn} values for even-even (top) and for even-Z, odd-N nuclei (bottom) at N~50 (based on Ref. 7).

Calculations of δV_{pn} using a simple zero-range δ–force [9] accounted for some of the experimental δV_{pn} values in the rare earth region but do not work for the actinides [10]. However, the recent first large-scale microscopic nuclear density-functional theory (DFT) calculations of δV_{pn} show nice agreement with the overall data trends and even the detailed behavior in certain mass regions [11]. These calculations are state-of-the-art and make predictions for new masses whose measurements would both provide interesting tests of them in new regions and also help to pinpoint degrees of freedom where the interactions used in these calculations might be improved.

In the vicinity of closed shells one can understand δV_{pn} values in terms of proton-neutron orbit occupations, nl_j, in the shell model. One example is given by the ^{208}Pb region. Figure 1 (left) shows empirical δV_{pn} values for this region. It is obvious that there are two trends for $N \leq 126$ nuclei. One of them can be defined for nuclei with $Z \leq 82$, for which the δV_{pn} values increase. This result is expected in terms of nl_j arguments: A shell for normal parity orbits begins with high j (angular momentum) and low n (principal quantum number) and ends with low j, high n. Therefore, just below the Z=82 and N=126 closed shells, protons and neutrons are filling similar nl_j orbits, the overlap between proton and neutron orbits is large, and large δV_{pn} values are expected. The opposite trend can be seen for nuclei with Z>82, which have decreasing δV_{pn} values. Here, low δV_{pn} values occur because the particles are filling dissimilar orbits. There is also a sudden increase just after N=126 in Fig. 1 (left), where protons and neutrons are added just above the Z=82 proton and N=126 neutron closed shells. Again, large δV_{pn} values are expected.

As shown in Fig. 1 (left), there is no data just after ^{208}Pb, i.e. there is no data for Z≤82 and N>126. This region corresponds to lower right quadrant in Fig. 1 (right). Low δV_{pn} values are expected in terms of orbit filling (protons will fill just below a shell, while neutrons are above the N=126 shell). With the availability of more data (i.e. mass values), a sudden decrease at N=128 for Z≤82 could be observed. At least, it is expected to see lower values than ~200 keV. To check this idea, new high-precision mass measurements in this region are required. One example is δV_{pn} (^{210}Pb), for which the ^{210}Pb, ^{208}Pb, and ^{206}Hg binding energies are already well-known, but as reported in the latest AME, the mass of ^{208}Hg is unknown. With a mass measurement of this nuclide it will be possible to calculate δV_{pn} (^{210}Pb), i.e. the very first δV_{pn} value in the lower quadrant in Fig. 1 (right), and thus be able to check the predictions mentioned above.

The N=56 region, especially for Zr and Mo, has an anomaly in the δV_{pn} results, which we cannot understand in terms of orbit filling. A down trend is seen for Mo, while an increase is observed for Zr at N=56 (see Fig. 2 (top)). Since four binding energies are required to calculate one δV_{pn} value, the anomaly can originate from any of these four. For even Z (or N) and odd N (or Z), there are similar spikes down and up for both Mo and Zr at N=55 (see Fig. 2 (bottom)). Since ^{94}Zr and ^{96}Zr are stable nuclei, their mass values are likely correct. Thus ^{95,97}Zr are of interest for new mass measurements. For more information see Ref. [7].

Figure 3 shows another color coded graph for the region Z=50-82 and N=82-126. If protons and neutrons have a similar fractional filling (f_p = Z/32, f_n= N/44), δV_{pn} values are expected and observed to be large along the diagonal line. Further away from the diagonal line, δV_{pn} values should be lower. ^{158}Sm is obviously anomalous in this sense: It has a low δV_{pn} value yet it lies near the diagonal line. To check this value, the ^{158}Sm, ^{156}Sm, ^{156}Nd, and ^{154}Nd mass-excess values are needed to a precision of at least 10 keV. Table 1 summarizes the known data and shows the need for further high-precision mass measurements.

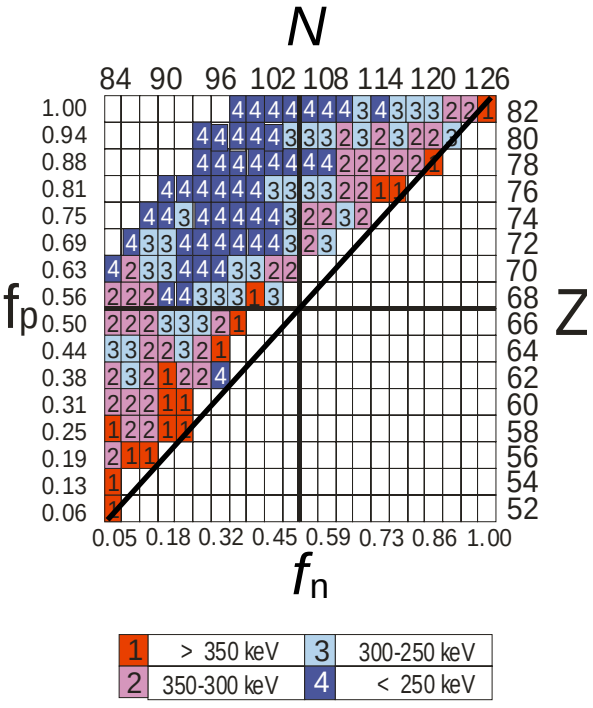

Figure 3: Empirical δV_{pn} values at the major shells Z=50-82, N=82-126 with proton and neutron fractional filling values (f_p and f_n) (based on Ref. 6).

Table 1: Four mass excess values related to $\delta V_{pn}(^{158}Sm)$. Mass excess taken from [5]

Nucleus	Mass excess (keV)	Uncertainty (keV)
^{158}Sm	-65210	80
^{156}Sm	-69370	10
^{156}Nd	-60530	200
^{154}Nd	-65690	110

Except for ^{156}Sm, the nuclides of interest have large mass uncertainties. Thus it may be that $\delta V_{pn}(^{158}Sm) = (250 \pm 61)$ keV is wrong. DFT calculations [11] give ~320 keV, which is a reasonable value along the diagonal line in Fig. 3. The value should be checked by measuring the ^{154} Nd, ^{156}Nd, and ^{158}Sm masses.

In summary, there are several reasons why particular δV_{pn} values should be measured. In some cases, the mass of the required nuclides is currently unknown and no δV_{pn} value can be determined. The aim is to find the first δV_{pn} value in the lower right quadrant of Fig. 3, which can be addressed with a new mass measurement of ^{208}Hg. Similar to the ^{208}Pb region, the ^{132}Sn mass region needs additional and new measurements. For example, ^{132}Cd is required to calculate $\delta V_{pn}(^{134}Sn)$. Furthermore, existing mass values may be wrong, possibly in the Mo mass region. Finally, some masses need to be determined to resolve differences between DFT calculations [11] and the present experimental data with respect to nuclear structure, as in the case of ^{158}Sm.

Experimental setup and overview of nuclides:

Mass measurements for the δV_{pn} study need to be performed with an uncertainty of about 10 keV, which corresponds to a relative uncertainty of below $\delta m/m=10^{-7}$ in the heavy mass region around A=200 for an individual nuclide mass. It can and has been provided so far only by Penning trap mass spectrometers like ISOLTRAP at ISOLDE/CERN [12].

With ISOLTRAP over 300 exotic nuclides have already been investigated, meanwhile reaching regularly a relative mass accuracy of the order of $\delta m/m=1\cdot10^{-8}$ [13]. Nuclides with production rates as low as 100 ions/s and half-lives well below 100ms can be addressed. The experimental setup and recent technical developments will be briefly introduced in the following:

ISOLTRAP employs three ion traps for the preparation and purification of radioactive ion bunches delivered by ISOLDE as well as for the measurement of the atomic mass. The 60-keV ISOLDE ion beam is first stopped, cooled, and bunched in a linear radio-frequency quadrupole (RFQ), which has an efficiency of up to 15%. Isobaric contaminants that are still present after mass selection with either the GPS or the HRS separator magnets, can be removed in the first, cylindrically shaped Penning trap: With an rf cyclotron excitation of the ion motion within a helium buffer-gas environment, the ions of interest can be mass-selected, reaching a resolving power of up to $m/\Delta m=10^5$. The isobarically pure ion bunch is then transferred to the hyperbolic precision Penning trap, where possible isomeric ions can be removed by application of a resonant dipolar rf excitation.

The mass measurement principle is based on the very precise determination of the cyclotron frequency $\nu_c=qB/(2\pi m)$ of ions with mass m and charge q that are stored in a strong and homogeneous magnetic field B. With the time-of-flight cyclotron-resonance technique the

gain of radial energy in the Penning trap after a quadrupolar rf excitation is probed by monitoring the change of the time of flight towards an external detector after axial ejection of the ions from the trap. The magnetic field strength is determined by measuring the cyclotron frequency of a reference ion with well-known mass. The mass of the ion of interest is finally deduced from the ratio of the two cyclotron frequencies. [14]

Within the last year several technical improvements have been realized at ISOLTRAP: The efficiency was increased by a factor of three by implementing a new detector that uses a Channeltron with a conversion dynode [15]. With the new detection efficiency of above 90% almost true single ion counting is possible. This gives better control of ion contamination and beam times can be used more efficiently. In addition, nuclides with even lower production yields can be addressed. The precision of the cyclotron frequency determination was also improved by a factor of about three, using time-separated oscillatory fields for the quadrupolar rf excitation in the precision trap (so-called Ramsey technique) [16]. The new method has been thoroughly tested for stable nuclides and was successfully applied in two on-line runs in 2006, when the masses of ^{38,39}Ca and ^{26,27}Al were measured with statistical uncertainties as low as $2 \cdot 10^{-9}$ within a few hours.

Closely related is the investigation of the temporal stability of the magnetic field strength. It was observed that the magnetic field strength, and thus the cyclotron frequency, depends on the temperature inside the warm bore of the magnet. A temperature regulation was installed in order stabilize the temperature to variations below +/-10mK. Finally, two new ion sources have been installed at ISOLTRAP: a new graphite oven with an additional gas cell including a filament for electron impact ionization in front of the RFQ buncher in order to deliver not only stable alkali ions but also stable ions of other elements including gaseous ions like helium, and a new carbon cluster ion source in front of the preparation Penning trap, in order to obtain carbon clusters as ideal reference masses. Both ion sources are in commissioning.

Those radionuclides that are of interest for the δV_{pn} study and which are accessible at ISOLTRAP are summarized in Table 2. In some cases a mass measurement can be scheduled and performed right away, while in other cases some target development is required. For nuclides with so far unmeasured production yields, further information is given below:

^{116,118,120}Pd:
In the ISOLDE yield data base there is only a yield given for ^{115}Pd, which was measured for a UC_x target and surface ionization. For the more neutron-rich nuclides lower yields are expected due to a slow diffusion of Pd out of the target. With a (to be developed) RILIS scheme a significantly higher ionization efficiency would help to boost the yields. In this case only In isotopes would remain as isobaric background. Further yield and target tests are thus required.

^{150}Ce, ^{154,156}Nd, ^{158,160}Sm:
For the Lanthanides the purity of the beam is likely a limiting factor. With ISOLTRAP a resolving power of more than 30000 can be achieved in the preparation Penning trap. Further yield measurements for a UC_x target with a CF_4 leak and possibly RILIS application for Nd and Sm are required.

$^{207\text{-}210}$Hg:
For the nuclide ^{207}Hg it is possible to use a standard molten Pb target with an MK3 ion source. More neutron-rich nuclides need to be produced with a UC_x target, supplied with a quartz transfer line in order to remove or reduce the contamination due to Fr. A RILIS scheme

for Hg is available at ISOLDE. The yields are expected to be above 10^3 ions/s, i.e. sufficient for a mass determination.

Table 2: Selection of radionuclides of interest (yields taken from the ISOLDE web page data base). For nuclides where no yield or target/ion source is given, some further information is mentioned in the text.

δV_{pn} nuclide	Nuclide to be measured	Half-life $T_{1/2}$	Target / ion source	est. Yield (at/μC)
^{72}Zn, ^{74}Zn	^{70}Ni	6 s	UC_x / RILIS	$1 \cdot 10^4$
^{84}Se, ^{86}Se	^{82}Ge	4.55 s	UC_x / HP	$7 \cdot 10^4$
^{118}Cd, ^{120}Cd	^{116}Pd	11.8 s		
^{120}Cd, ^{122}Cd	^{118}Pd	1.9 s		
^{122}Cd, ^{124}Cd	^{120}Pd	0.5 s		
^{125}In, ^{126}Sn, ^{122}Cd, ^{124}Cd	^{122}Cd	5.24 s	UC_x / RILIS	$3.5 \cdot 10^7$
^{125}In, ^{126}Sn, ^{128}Sn, ^{124}Cd, ^{126}Cd	^{124}Cd	1.25 s	UC_x / RILIS	$7.7 \cdot 10^6$
^{128}Sn, ^{130}Sn, ^{126}Cd	^{126}Cd	0.52 s	UC_x / RILIS	$8.9 \cdot 10^5$
^{130}Sn, ^{132}Sn	^{128}Cd	0.28 s	UC_x / RILIS	$1.3 \cdot 10^5$
^{132}Sn, ^{134}Sn	^{130}Cd	162 ms	UC_x / RILIS	$1 \cdot 10^4$
^{134}Sn	^{134}Sn	1.12 s	UC_x / HP+^{34}S	$1 \cdot 10^5$
^{138}Xe, ^{142}Ba	^{138}Xe	14.1 m	UC_x / CP	$5.7 \cdot 10^8$
^{142}Ba	^{140}Xe	13.6 s	UC_x / CP	$3.5 \cdot 10^8$
^{152}Nd	^{150}Ce	4.0 s		
^{158}Sm	^{154}Nd	25.9 s		
^{158}Sm	^{156}Nd	5.5 s		
^{158}Sm	^{158}Sm	5.3 m		
^{162}Gd	^{160}Sm	9.6 s		
^{209}Pb	^{207}Hg	2.9 m		
^{210}Pb, ^{211}Pb, ^{212}Pb	^{208}Hg	~ 42 m		
^{211}Pb	^{209}Hg	37 s		
^{212}Pb	^{210}Hg			
^{225}Ra	^{223}Rn	24.3 m	UC_x / CP	$2.5 \cdot 10^6$
^{227}Ra	^{224}Rn	107 m	UC_x / CP	$2.8 \cdot 10^6$
^{227}Ra	^{225}Rn	4.7 m	UC_x / CP	$1.7 \cdot 10^5$

Beam time request:

In Table 3 a list of nuclides is given, indicating which masses we would like to measure in the next two years that are relevant for the δV_{pn} study. We have divided the list in two parts; those masses which we would like to address first, since they are readily available at ISOLDE (**) and those for which further yield measurements and target tests are required (*). In some cases there is an overlap to a previous proposal for mass measurements or to a new proposal on trap-assisted spectroscopy, indicated by an asterisk at the number of shifts. For the remaining new cases we ask for 14 shifts of beam time.

Table 3: Overview of radionuclides, for which shifts are requested in this proposal. The nuclides are separated into two groups with respect to their availability at ISOLDE. Beam-time shifts marked with an asterisk overlap with a previous proposal or another new proposal. The runs for the Xe and Rn isotopes can be merged into one beam time.

Nuclides	No. of shifts	Available	Target	ion source
2008-2009: 14 radioactive beam shifts				
^{82}Ge	3	**	UC_x / n conv.	HP
^{134}Sn	3	**	UC_x / ^{34}S	HP
^{138,140}Xe	3	**	UC_x	CP
$^{223-225}$Rn	5	**	UC_x	CP
2008-2009: 7 radioactive beam shifts (part of new proposal on trap-assisted spectroscopy)				
$^{207-210}$Hg	*	**	UC_x / quartz	RILIS
2007-2008: 10 radioactive beam shifts (already allocated for proposal P160)				
^{70}Ni	*	**	UC_x / all graphite	RILIS
^{122,124,126,128,130}Cd	*	**	UC_x / quartz / n conv.	RILIS
target tests required				
^{116,118,120}Pd		*	UC_x	RILIS
^{150}Ce		*	UC_x / CF_4	
^{154,156}Nd		*	UC_x / CF_4	RILIS
^{158,160}Sm		*	UC_x / CF_4	RILIS

References:

[1] I. Talmi, Rev. Mod. Phys. 34, 704 (1962)
[2] K. Heyde et al., Phys. Lett. 155B, 303 (1985)
[3] P. Federman and S. Pittel, Phys. Lett. 69B, 385 (1977) ; Phys. Lett. B 77, 29 (1978)
[4] J.-Y. Zhang et al., Proc. Int. Conf. Cocoyoc, Mexico C65, 109 (1988); J.-Y. Zhang, R.F. Casten, and D.S. Brenner, Phys. Lett. B 227, 1 (1989)
[5] G. Audi, A.H. Wapstra, and C. Thibault, Nucl. Phys. A729, 337 (2003)
[6] R.B. Cakirli, D.S. Brenner, R.F. Casten, E.A. Millman, Phys. Rev. Lett., 94, 092501 (2005); R.B. Cakirli, D.S. Brenner, R.F. Casten, E.A. Millman Phys. Rev. Lett. 95, 119903(E) (2005)
[7] D.S. Brenner, R.B. Cakirli, and R.F. Casten, Phys. Rev. C 73, 034315 (2006)
[8] R.B. Cakirli, R.F. Casten, Phys. Rev. Lett. 96, 132501 (2006)
[9] Y. Oktem et al., Phys. Rev. C 74, 027304 (2006)
[10] R.F. Casten, R.B. Cakirli, private communication
[11] M. Stoitsov, R.B. Cakirli, R.F. Casten, W. Nazarewicz, and W. Satula, Phys. Rev. Lett. 98, 132502 (2007)
[12] G. Bollen et al., Nucl. Instrum. and Meth. A 368 (1996) 675; F. Herfurth et al., J. Phys. B: At. Mol. Opt. Phys. 36 (2003) 931.
[13] A. Kellerbauer et al., Eur. Phys. J. D 22, 53 (2003)
[14] K. Blaum, Phys. Rep. 425, 1 (2006)
[15] C. Yazidjian et al., Hyperfine Interact., in press
[16] S. George et al., Phys. Rev. Lett. 98, 162501 (2007); S. George et al., Int. J. Mass Spectrom., accepted; M. Kretzschmar, Int. J. Mass Spectrom., accepted